

ACTIVE FLOW CONTROL BUMP DESIGN USING HYBRID NASH-GAME COUPLED TO EVOLUTIONARY ALGORITHMS

D. S. Lee^{*}, J. Periaux[†], L. F. Gonzalez^{††}, K. Srinivas^{†††} and E. Onate[†]

^{*}CIMNE/UPC and AMME/Univ. of Sydney

Parque Mediterraneo de la Tecnologia (PMT), Edificio C3 CIMNE, 08860 Castelldefels, Spain

e-mail: ds.chris.lee@gmail.com.

[†]International Center for Numerical Methods in Engineering (CIMNE)

Edificio C1, Gran Captian, s/n. 08034 Barcelona, Spain.

e-mail: jperiaux@gmail.com, onate@cimne.upc.edu.

^{††}Engineering System, Queensland University of Technology

Brisbane, Australia.

e-mail: felipe.gonzalez@qut.edu.au.

^{†††} Aerospace Mechanical & Mechatronics Engineering (AMME), University of Sydney

Sydney, NSW 2006 Australia.

e-mail: k.srinivas@usyd.edu.au.

Key words: Active Flow Control, CFD, Shape Optimisation, Evolutionary Algorithm, Nash-Game

Abstract. *In this paper, the optimal design of an active flow control device; Shock Control Bump (SCB) on suction and pressure sides of transonic aerofoil to reduce transonic total drag is investigated. Two optimisation test cases are conducted using different advanced Evolutionary Algorithms (EAs); the first optimiser is the Hierarchical Asynchronous Parallel Evolutionary Algorithm (HAPMOEA) based on canonical Evolutionary Strategies (ES). The second optimiser is the HAPMOEA is hybridised with one of well-known Game Strategies; Nash-Game. Numerical results show that SCB significantly reduces the drag by 30% when compared to the baseline design. In addition, the use of a Nash-Game strategy as a pre-conditioner of global control saves computational cost up to 90% when compared to the first optimiser HAPMOEA.*

1 INTRODUCTION

With rising fuel price and increasing environmental issues, the drag reduction of transonic civil aircraft is emerging as one of most important aeronautical problems. Such drag reduction allows improving fuel efficiency which is directly related to aircraft emissions. Recent advances in design tools, materials, electronics and actuators offer implementation of flow control technologies on current transonic aircraft that can

improve aerodynamic efficiency. In addition, the use of active flow control devices can save manufacturing time/cost without replacement of current airfoil or wing planform shape [1 -3].

The paper investigates a Shock Control Bump (SCB) active flow control technique which controls flow behaviour over aerofoil at transonic speeds [3, 4]. The main objective of using SCB is to decelerate supersonic flow and delay shock occurrence.

In this paper, the SCB shape design is considered at critical flight conditions where shock is occurred on both upper and lower surfaces of a typical transonic aerofoil; RAE 2822. Two practical optimizations are conducted using two different optimisation methods; the first uses Hierarchical Asynchronous Parallel Evolutionary Algorithms (HAPMOEA) which is based on the concept of hierarchical multi-population with multi-resolution. In the second optimiser, HAPMOEA is hybridized with Nash-Game instead of using hierarchical multi-population which denoted herein as Hybrid-Game. The major role of Nash-Game is the decomposition of the design problem, for instance, a complex multi-objective design problem will be split into several simpler single-objective design problems respect to Nash-Players. Because of this characteristic Nash-Players can act as a pre-conditioner of a global optimizer [5 -7].

The paper will show how to design optimal SCB to control the flow over aerofoil and also demonstrate how Hybrid-Game improves optimisation efficiency.

The rest of paper is organized as follows; Section 2 describes optimisation methods HAPMOEA and Hybrid-Game. The aerodynamic analysis tool for SCB design optimisation is described in Section 3. Section 4 considers SCB design optimisation using HAPMOEA and Hybrid-Game coupled to EA. Finally Section 5 presents conclusions and future research.

2 OPTIMISATION METHODS

The evolutionary algorithm used in this paper is based on Covariance Matrix Adaptation Evolutionary Strategies (CMA-ES) [8]. It also incorporates Distance Dependent Mutation and asynchronous parallel computation at the core of algorithm [9 -11].

The first method HAPMOEA uses the concept of multi-population/fidelity hierarchical topology which can provide different models including precise, intermediate and approximate models [12] as shown in Figure 1 a).

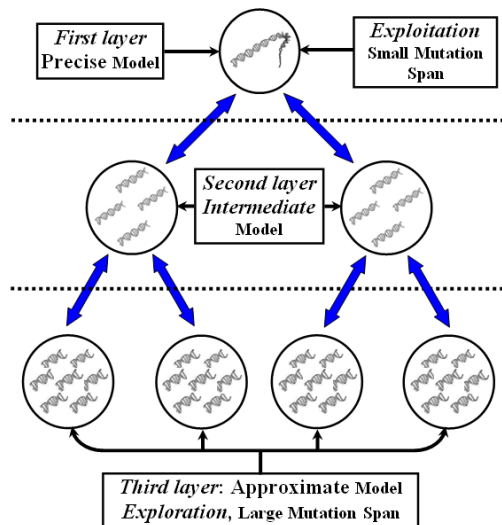


Figure 1 a). Hierarchical multi-population topology.

Each node/population (Node0 ~ Node6) belonging to the different hierarchical layer can be handled by a different EA code.

The second method hybridises HAPMOEA by applying a concept of Nash-Equilibrium instead of the concept of hierarchical topology which is denoted as Hybrid-Game. Figure 1 b) shows one example topology for Hybrid-Game which consists of three Nash-Players and one Global-Player. The Hybrid-Game takes a high fidelity/resolution population from HAPMOEA to the core of Nash-Game hence; the Nash-Players can seed/update their elite designs to Global-Player (Node0).

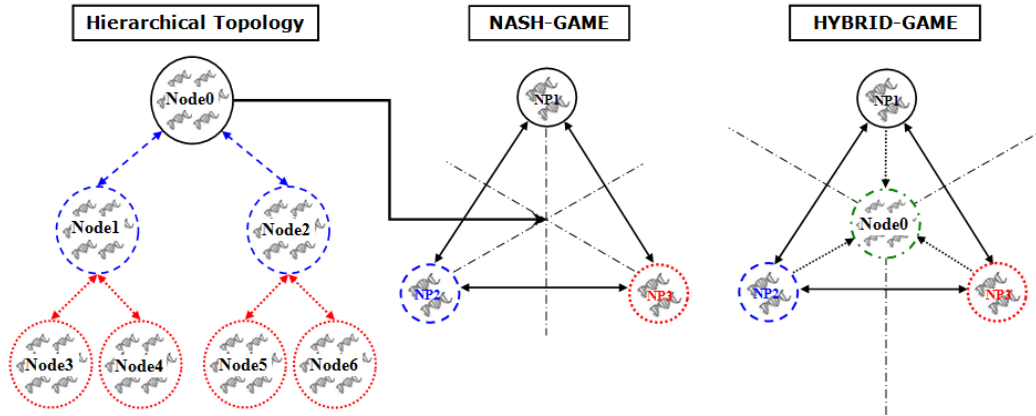


Figure 1 b). Example topology for Hybrid-Game.

The Nash-Game players choose their own strategy to improve their own objective. In this paper, both HAPMOEA and Hybrid-Game are coupled to the aerodynamic analysis tool for double SCB design optimisation. Details and validations of HAPMOEA and Hybrid-Game can be found in references [5, 6, 12].

3 AERODYNAMIC ANALYSIS TOOL

In this paper the Euler - Boundary layer code MSES written by Drela [13] is utilised. The MSES software is a coupled viscous/inviscid Euler method for the analysis and design of multi-element or single-element airfoils. It is based on a streamline-based Euler discretization and a two-equation integral boundary layer formulation are coupled through the displacement thickness and solved simultaneously by a full Newton method. To obtain a prescribed lift coefficient C_l , the angle of attack α of the airfoil is adapted. Figure 2 shows an example of a mesh obtained by MSES that used during the optimisation.

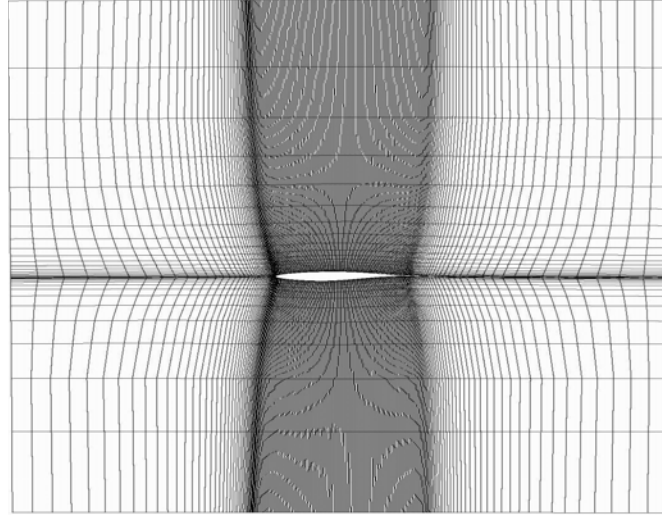
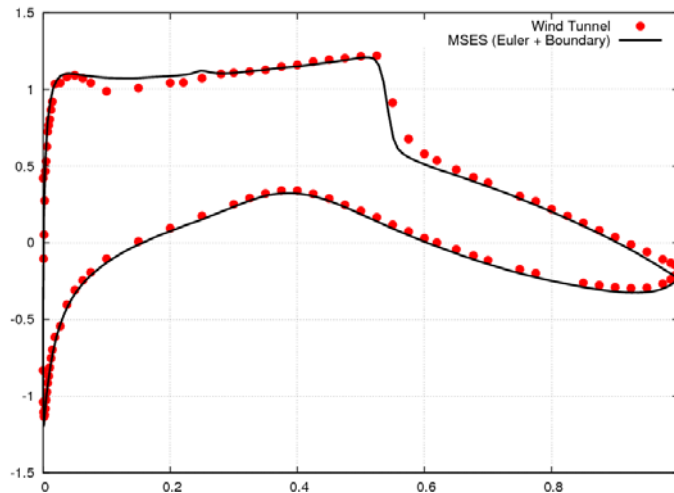


Figure 2. RAE 2822 aerofoil mesh obtained by MSES.

3.1 Validation of MSES

A validation test is conducted on a 4×2.8 GHz CPU. The flow conditions are Mach number (M_∞) = 0.729, angle of attack (α) = 2.31° and Reynolds number (Re) = 6.5×10^6 . Figure 3 compares the results obtained by MSES to the wind tunnel experimental data [14]. It can be seen there is good agreement between C_p distribution obtained from MSES and the wind tunnel data.

Figure 3. C_p distribution obtained by MSES and wind tunnel experiment data.

4 SHOCK CONTROL BUMP ON TRANSONIC AEROFOIL

At transonic speeds, the flow over the high camber wing causes shock waves where there is a large amount of gas property changes and the flow becomes irreversible. Through the shock, total pressure decreases and entropy increases which means there is a loss of energy. In other words, there is an increment of wave drag. To cope with this problem, Ashill *et al.* 1992 [3] proposed the concept of a transonic bump named Shock Control Bump (SCB) by using geometry adaption on an aerofoil. As illustrated in Figure 4, the SCB can be constructed using design variables: length, height and peak position. The middle of SCB will be located at where the shock occurs on the transonic aerofoil design.

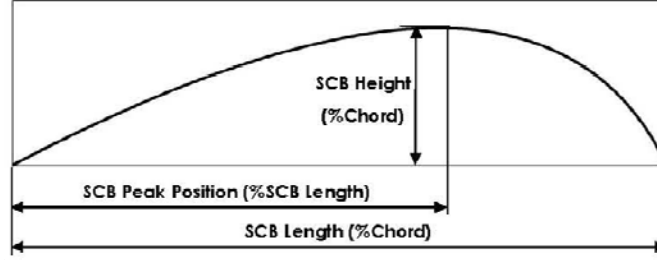
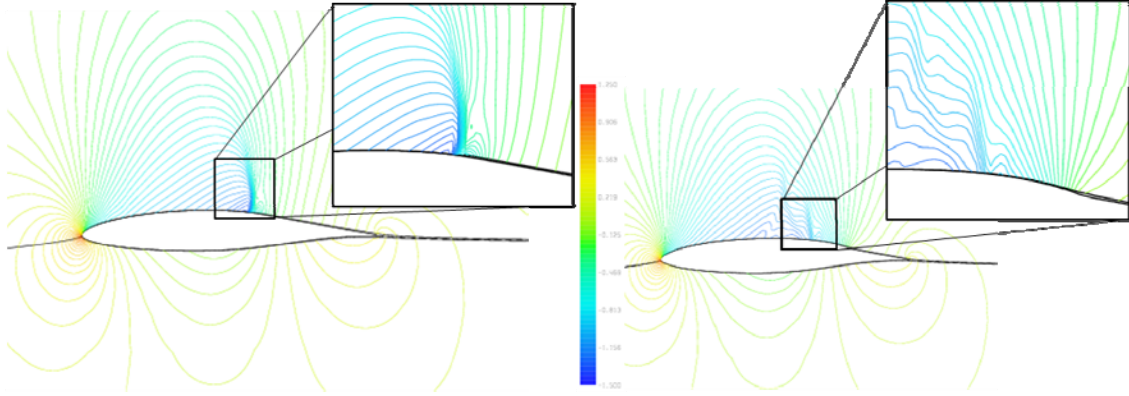


Figure 4. SCB design components.

Figure 5 illustrates the concept and benefit of using a SCB. The transonic flow over normal aerofoil without SCB accelerates to supersonic and the pressure forms a strong shock that leads a high Cd_{wave} is shown in Figure 5 (a). However the pressure difference over the SCB causes the supersonic flow to decelerate to subsonic Mach numbers by isentropic compression waves is shown in Figure 5 (b). This leads to significant wave drag reduction.


Figure 5 a). C_p contour for baseline design. Figure 5 b). C_p Contour for baseline design with SCB.

In the following section, the shape of double SCB on the suction and pressure sides of the RAE2822 aerofoil is optimized using HAPMOEA and Hybrid-Game to minimize the total drag as shown in Equation (1);

$$f(U_SCB, L_SCB) = \min(Cd_{Total}) \quad (1)$$

$$\text{Stopping criteria; } Cd_{Total} \leq 0.01285$$

where U_SCB, L_SCB represent a set of design variables for SCB on upper and lower surfaces of RAE 2822.

The design bounds are shown in Table 1 where the peak position is represented as percentage of SCB length. Six design variables are considered for the optimisation.

SCB Bounds	Length (%c)	Height (%c)	Peak Position
Lower	15.0	0.35	0.5
Upper	30.0	0.65	0.85

Table 1. SCB design bounds for optimisation.

5 SCB DESIGN OPTIMISATION USING HAPMOEA AND HYBRID-GAME

The baseline design (RAE 2822) is shown in Figure 6 a). The problem considers the critical flow conditions; $M_\infty = 0.8$, $C_l = 0.175$, $Re = 18.63 \times 10^6$ where two shocks occur, one in the suction side and one in the pressure side of RAE 2822 as shown in Figure 6 b).

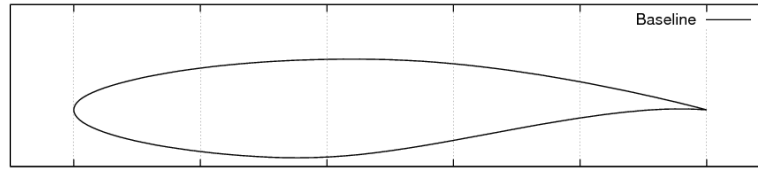


Figure 6 a). Baseline design (RAE 2822) aerofoil.

It can be seen that the upper and lower sonic points occur at 70.6% and 51.3% of chord respectively. In the following subsections, double SCB design optimization using HAPMOEA and Hybrid-Game are conducted to minimize the total drag (Cd_{Total}). The aerodynamic analysis tool; MSES will run twice for each function evaluation; the first run will analyse the upper SCB and the second run will analyse both the upper and lower SCB.

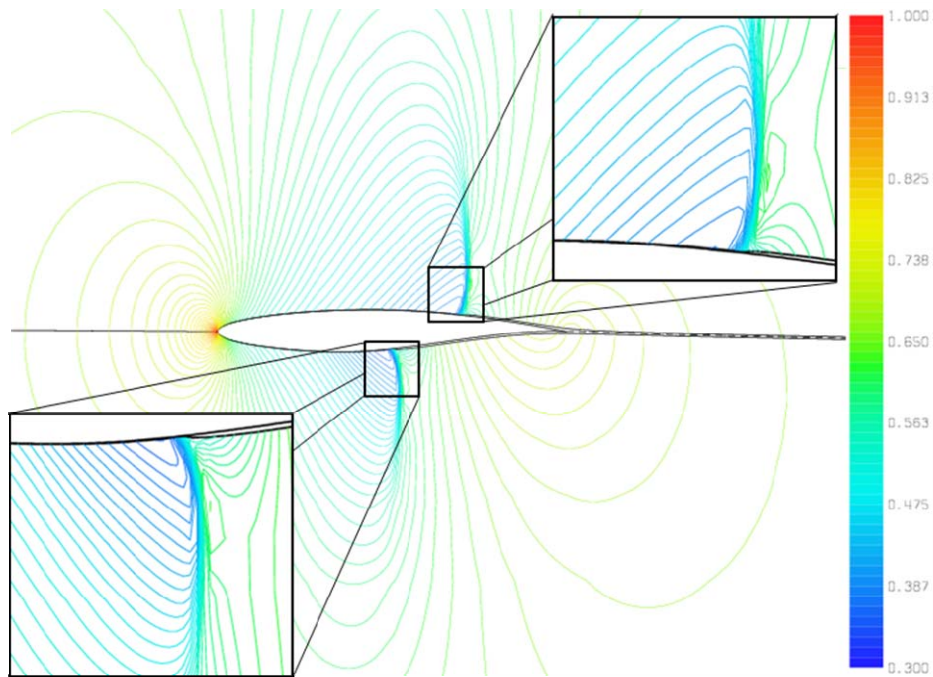


Figure 6 b). P/P_0 contour obtained by baseline design.

5.1 SCB Design using HAPMOEA

Problem Definition

The problem considers a single-objective SCB design optimisation using HAPMOEA to minimize total drag (Eq. (1)) at flow conditions; $M = 0.8$, $C_l = 0.175$, $Re = 18.63 \times 10^6$. Figure 7 shows the evaluation mechanism for HAPMOEA which consists of hierarchical multi-population (Node 0 ~ Node 6) based on multi-resolution. Each individual will be analysed twice with the aerodynamic analysis tool to evaluate the double SCB design at different resolution layers (precise, intermediate and less fine).

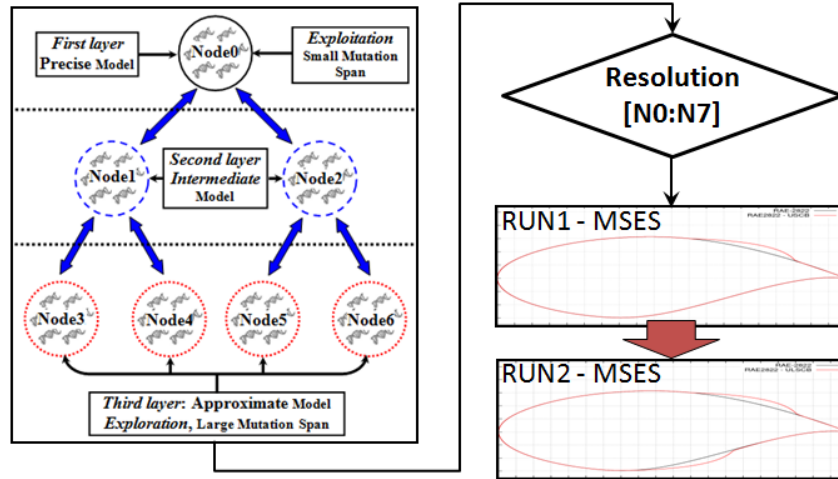


Figure 7. Evaluation mechanism for HAPMOEA.

Implementation

The following conditions are for multi-resolution/population hierarchical populations.

- 1st Layer: Population size of 10 with a computational grid of 36×213 points (Node0).
- 2nd Layer: Population size of 20 with a computational grid of 24×131 points (Node1, Node2).
- 3rd Layer: Population size of 20 with a computational grid of 24×111 points (Node3 ~ Node6).

Note: these grid conditions (2nd and 3rd layer) produce less than a 5% accuracy error when compared to the precise model on the 1st layer (Node0).

Interpretation of Numerical Results

As illustrated in Figure 8, the algorithm was allowed to run for 12 hours and 1,295 function evaluations ($f = 0.01285$) using a single 4×2.8 GHz processor. Table 2 compares the aerodynamic characteristics obtained by the baseline design (RAE 2822) and baseline with optimal SCB. It can be seen that the baseline design with optimal SCB can reduce wave drag by 75% which leads to 33% of total drag. Such drag reduction improves 49% of the lift to drag ratio.

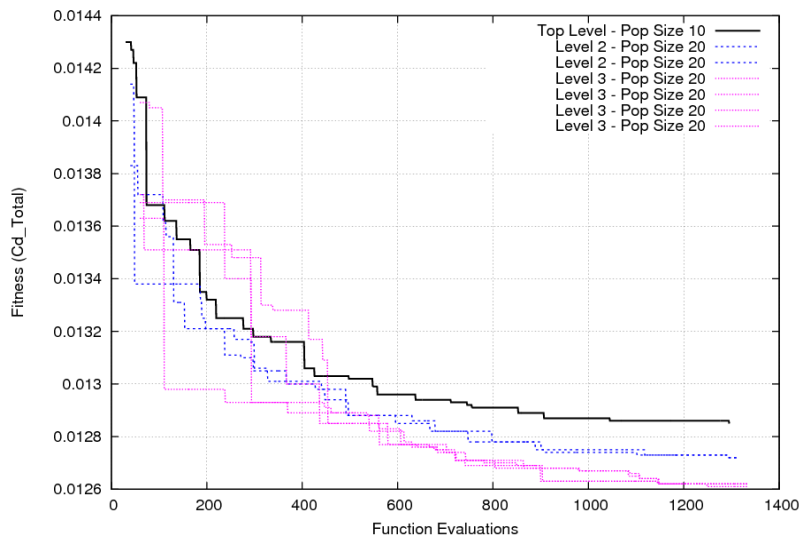


Figure 8. Convergence objective obtained by HAPMOEA.

SCB	Cd_{Total}	Cd_{Wave}	L/D
Baseline	0.01918	0.00886	9.13
with SCB	0.01285 (- 33%)	0.00225 (- 75%)	13.59 (+ 49%)

Table 2. Aerodynamic characteristics obtained by HAPMOEA.

Figure 9 compares the shape of baseline design and baseline with SCB geometry. The optimal SCBs obtained by HAPMOEA are located between (0.5604, 0.0595) and (0.8506, 0.0270) on the suction side and between (0.3633, -0.0591) and (0.6618, -0.0287) on the pressure side. The design parameters for the optimal SCB are shown in Table 3.

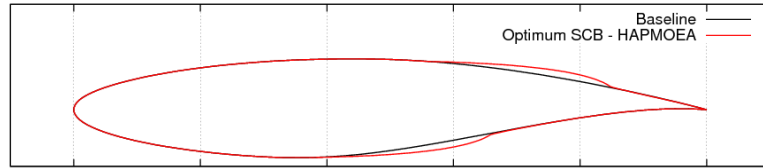


Figure 9. Geometries comparison between the baseline design and baseline with SCB.

SCB	Length (%c)	Height (%c)	Peak Position
Upper	29.02	0.603	83.8
Lower	29.85	0.643	84.8

Table 3. SCB design parameters obtained by HAPMOEA (Note: Peak Position is in % of SCB length).

Figure 10 compares the C_p distributions obtained by the baseline design and baseline with optimal SCB. It can be seen that both upper and lower SCB decelerates the supersonic flow and the position of the shock is moved towards to trailing edge. Using only an upper optimal SCB reduces the total drag by 14% while applying both upper and lower optimal SCB produces 33% lower total drag when compared to the baseline design.

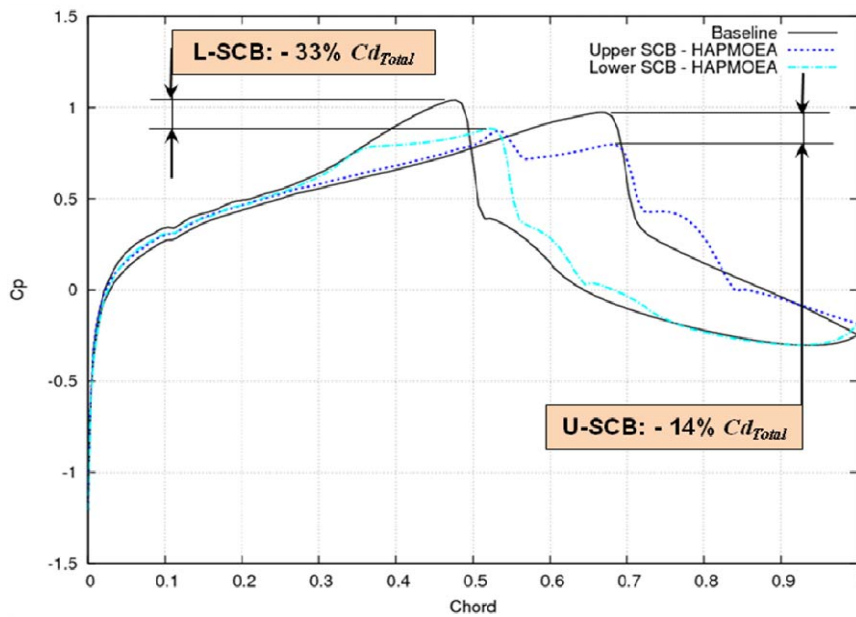


Figure 10. C_p distributions obtained by the baseline design and with SCB.

5.2 SCB Design using Hybrid-Game

Problem Definition

The problem considers single-objective SCB design optimisation using Hybrid-Game employing one Global-Player and two Nash-Players. Therefore the fitness function Eq. (1) becomes Equations (2), (3) and (4) due to the Nash-Players;

$$f_{GP}(U_SCB, L_SCB) = \min(Cd_{Total}) \quad (2)$$

$$f_{NP1}(U_SCB, L_SCB^*) = \min(Cd_{Total}) \quad (3)$$

$$f_{NP2}(U_SCB^*, L_SCB) = \min(Cd_{Total}) \quad (4)$$

where U_SCB^* and L_SCB^* represent the elite SCB designs obtained by Nash-Player 1 and Nash-Player 2 respectively.

Figure 11 shows the evaluation mechanism for Hybrid-Game which employs three players; Global-Player and Nash-Player 1 and 2. The Global-Player runs the aerodynamic analysis tool twice since its optimisation domain includes both upper and lower SCB. However, the analysis tool is run once for each Nash-Player 1 and 2 due to the Nash-Game decomposition characteristics. Nash-Player 1 (Eq. (3)) will only optimize a SCB on the suction side with an elite lower SCB obtained by Nash-Player 2 while Nash-Player 2 (Eq. (4)) will optimise a SCB on the pressure side using an elite upper SCB design from Nash-Player 1 shown in Eq. (4). The elite designs obtained by Nash-Players will be seeded to the Global-Player population. This optimisation mechanism allows the acceleration of the optimisation process of the Global-Player.

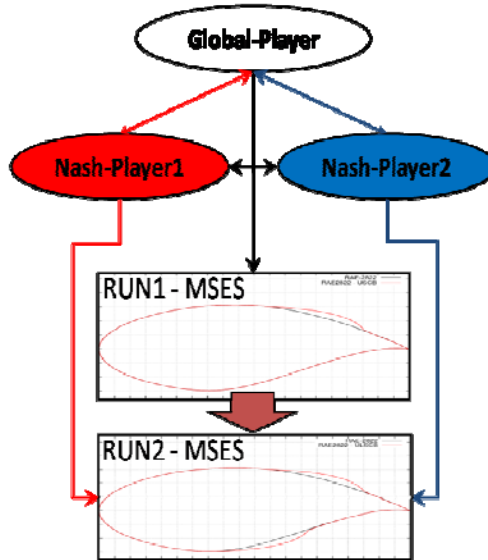


Figure 11. Evaluation mechanism for Hybrid-Game.

Implementation

The conditions for Hybrid-Game are;

- Global Player: Population size of 10 with a computational grid of 36×213 points.
- Nash-Player 1: Population size of 10 with a computational grid of 24×131 points.
- Nash-Player 2: Population size of 10 with a computational grid of 24×131 points.

Interpretation of Numerical Results

The algorithm runs for 1.15 hours and 406 function evaluations to reach same fitness function value ($f = 0.01282$) as with the first optimisation method (Section 5.1) using a single 4×2.8 GHz processor. Figure 12 (a) shows the convergence objective obtained by Hybrid-Game and also compares the computational cost obtained by HAPMOEA and Hybrid-Game. The computational cost for Hybrid-Game is only 9.5% of HAPMOEA computation cost due to Nash-Game characteristics (decomposition of design problem) and evaluation mechanism. In other words, the use of Nash-Game besides hierarchical topology improves the MOEA efficiency by 90%. In addition, the Hybrid-Game produces slightly better solution even though it has lower computational cost. Table 4 compares the aerodynamic characteristics obtained by the baseline design (RAE 2822) and baseline with optimal SCB. It can be seen that the baseline design with optimal SCB can reduce wave drag by 76% which leads to 33% of total drag. Such drag reduction improves 50% of the lift to drag ratio.

SCB	Cd_{Total}	Cd_{Wave}	L/D
Baseline	0.01918	0.00886	9.13
with SCB	0.01282 (- 33%)	0.00214 (- 76%)	13.65 (+ 50.0%)

Table 4. Aerodynamic characteristics obtained by Hybrid-Game.

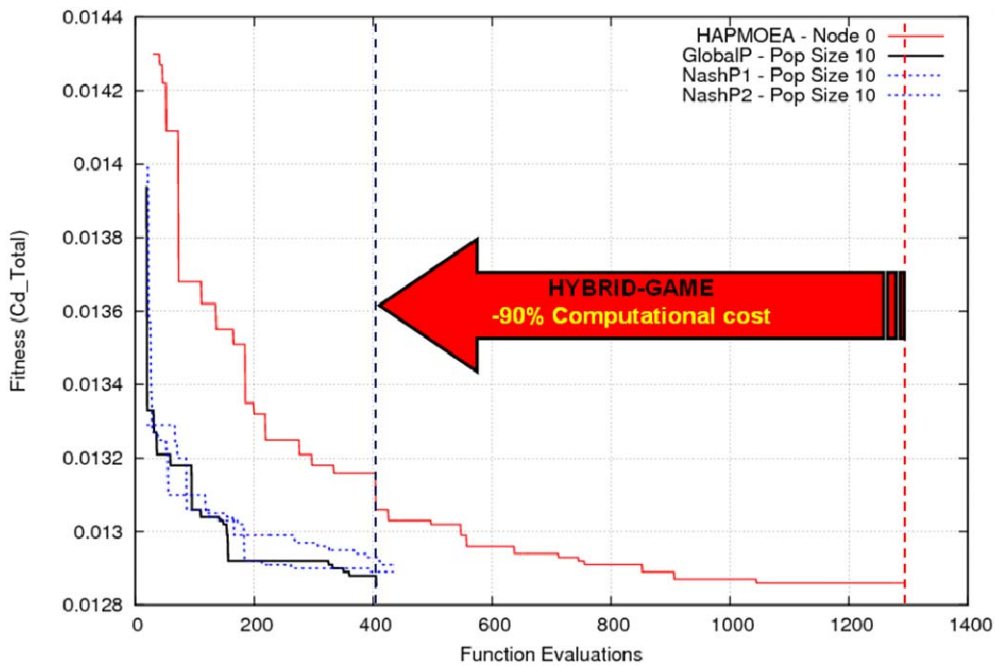


Figure 12. Convergence objective obtained by Hybrid-Game.

Figure 13 compares the shape of baseline design and baseline with SCB geometry obtained by Hybrid-Game. The optimal double SCB are located at between (0.5566, 0.0597) and (0.8543, 0.0263) on the suction side, and between (0.3624, -0.0591) and (0.6619, -0.0287) on the pressure side of RAE 2822. The design parameters for optimal SCB are described in Table 3.

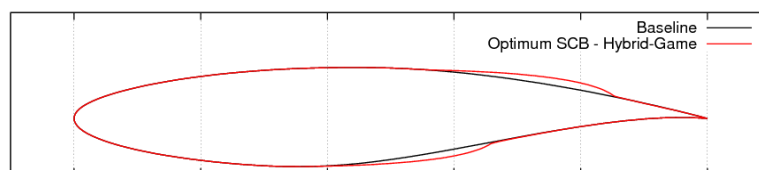
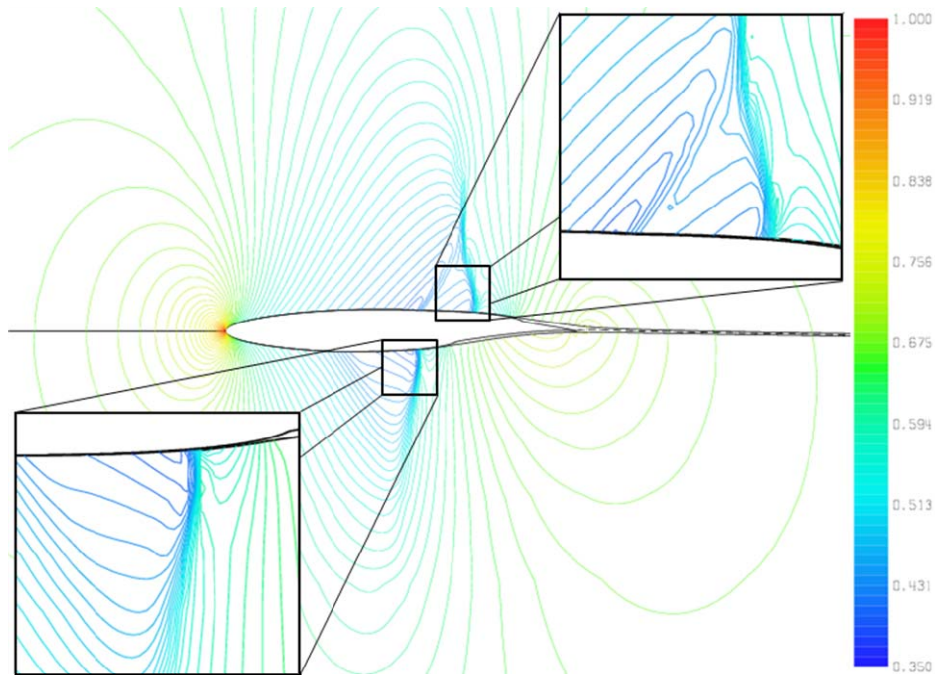


Figure 13. Geometries comparison between the baseline design and baseline with SCB.

SCB	<i>Length (%c)</i>	<i>Height (%c)</i>	<i>Peak Position</i>
Upper	29.77	0.644	84.8
Lower	29.94	0.643	84.8

Table 5. SCB design parameters obtained by Hybrid-Game (Note: *Peak Position* is in % of SCB length).

Figure 14 compares C_p contours obtained by the baseline design and baseline with optimal SCB. It can be seen that both upper and lower SCB decelerates the supersonic flow and the position of shock is moved towards to trailing edge when compared to the baseline design shown in Figure 6 (b). Using only upper optimal SCB reduces the total drag by 14% while applying both upper and lower optimal SCB produces 33% lower total drag when compared to the baseline design.

Figure 14. P/P_0 contour obtained by Hybrid-Game.

Figures 15 (a) and (b) compare the total drag (Cd_{Total}) and wave drag (Cd_{Wave}) distributions obtained by the baseline design and baseline with the optimal SCB found by HAPMOEA and Hybrid-Game. The flow conditions are; $M_\infty \in [0.5:0.85]$ with $Cl_{Fixed} = 0.175$, $Re = 18.63 \times 10^6$. The optimal SCB from Hybrid-Game performs similar to HAPMOEA and starts to produce lower total drag when Mach is higher than 0.77. One thing should be noticed from Figure 15 (b) is that the critical Mach number ($M_C = 0.75$) for the baseline design is extended to Mach number 0.77.

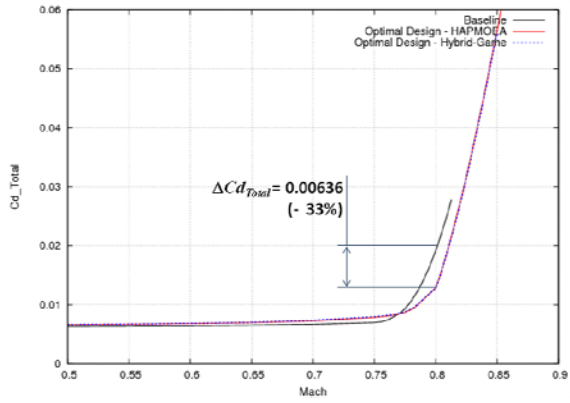


Figure 15 a) Cd_{Total} vs. Mach.

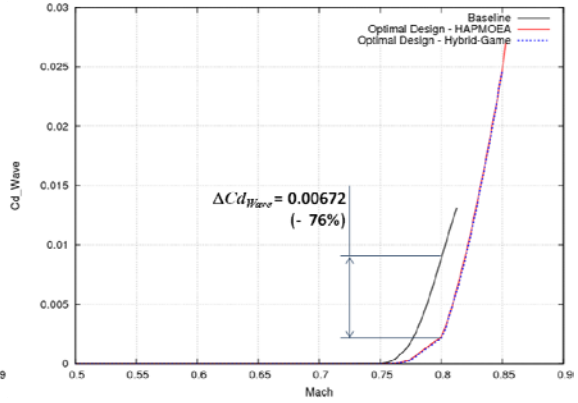


Figure 15 b). Cd_{Wave} vs. Mach.

Figure 16 compares the total drag distribution obtained by the baseline design and baseline with the optimal SCB found by HAPMOEA and Hybrid-Game for $Cl \in [0.1:0.85]$ with $Cl_{Fixed} = 0.175$, $Re = 18.63 \times 10^6$. Both optimal SCB from HAPMOEA and Hybrid-Game produce lower drag for a range of Cl values when compared to the baseline design. In addition, the optimal SCB from Hybrid-Game has slightly lower total drag when compared to the optimal SCB obtained by HAPMOEA even though the Hybrid-Game ran only 9.5% of HAPMOEA computation cost.

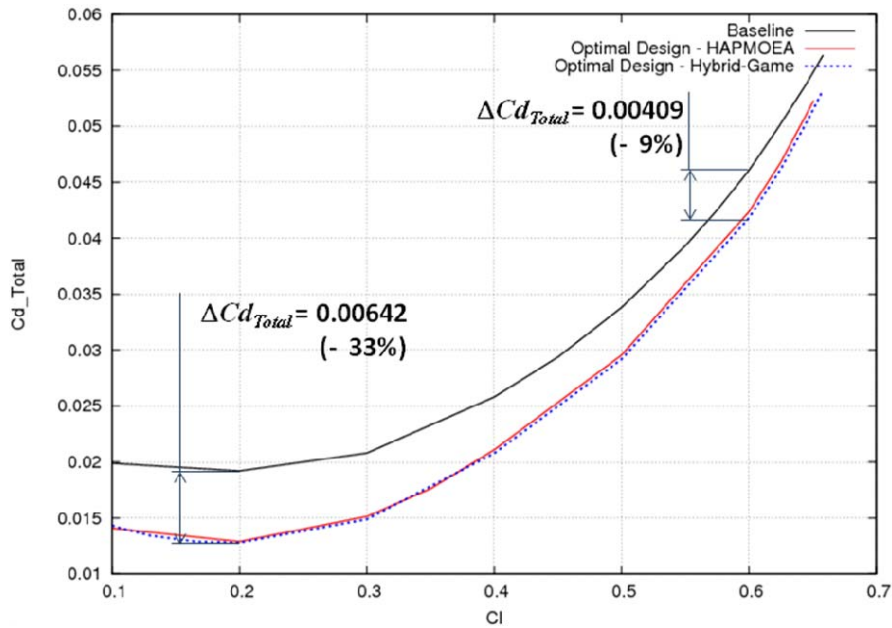


Figure 16. Cd_{Total} vs. Cl .

This optimal double SCB is also tested at five different flight conditions to show the benefit of using a double SCB. The histogram shown in Figure 17 shows the comparison of total drag and the ratio of lift to drag obtained by the baseline design and optimal double SCB from HAPMOEA and Hybrid-Game. It can be seen that the optimal double SCB at critical flight conditions reduces more total drag by 15 to 33% and improves lift to drag ratio by 18 to 49% at normal flight conditions when compared to the baseline design.

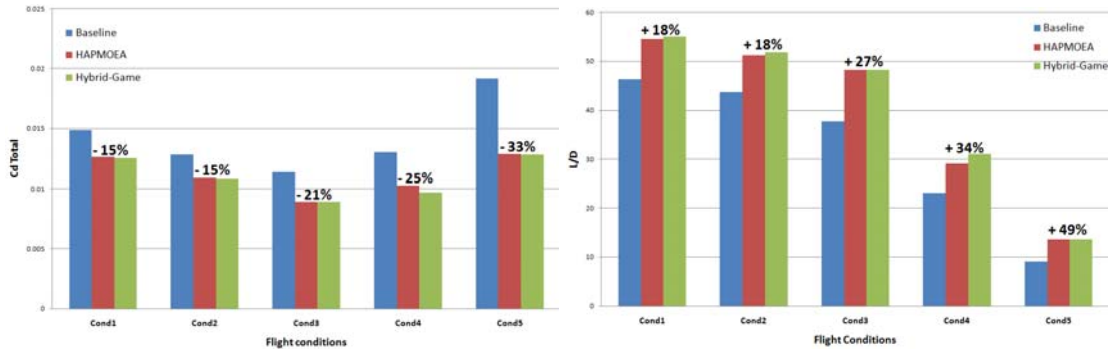


Figure 17. Drag reduction and lift to drag ratio improvement at normal flow conditions.

Note: $Cond_i$ represents i th flow conditions.

$Cond_1$: $M_\infty = 0.750$, $Cl = 0.690$, $Re = 18.63 \times 10^6$, $Cond_2$: $M_\infty = 0.760$, $Cl = 0.560$, $Re = 18.63 \times 10^6$

$Cond_3$: $M_\infty = 0.770$, $Cl = 0.430$, $Re = 18.63 \times 10^6$, $Cond_4$: $M_\infty = 0.785$, $Cl = 0.300$, $Re = 18.63 \times 10^6$

$Cond_5$: $M_\infty = 0.800$, $Cl = 0.175$, $Re = 18.63 \times 10^6$

To summarise the optimisation test case, the use of optimal SCB obtained by HAPMOEA and Hybrid-Game is beneficial at both normal and critical flow conditions due to significant transonic drag reduction. In addition, Hybrid-Game improves MOEA efficiency while generating high quality optimal solution when compared to HAPMOEA.

6 CONCLUSION

In this paper, two advanced optimisation techniques have been described and implemented as a methodology for active flow control bump named Shock Control Bump shape design optimisation. Analytical research clearly shows the benefits of coupling a Hybrid-Game to a MOEA in terms of computational cost and design quality. In addition, the use of SCB on current aerofoil reduces transonic drag significantly. In long term view, the use of SCB will save not only operating cost but also critical aircraft emissions due to less fuel burn.

Future work will focus on robust design optimization of SCB (Taguchi method) which can produce the model with better performance and stability at variability of operating conditions and transition positions.

ACKNOWLEDGEMENT

The authors gratefully acknowledge Eric J. Whitney, and M. Sefrioui, Dassault Aviation for fruitful discussions on Hierarchical EAs and their contribution to the optimisation procedure and, also to M. Drela at MIT for providing *MSES* software.

REFERENCES

- [1] H. Bart-Smith, and P. E. Risseuw, High Authority Morphing Structures, in Proceedings of IMECE 03, no. IMECE 2003-43377, (Washington, D.C), 2003 ASME International Mechanical Engineering Congress, November (2003)
- [2] R. Oborn, S. Kota, and J. A. Hetrick, Active Flow Control Using High-Frequency Compliant Structures. *Journal of Aircraft*, Vol. 41, No. 3, pp 603-609. (2004)
- [3] P. R. Ashill, L. J. Fulker, and A. Shires, A novel technique for controlling shock strength of laminar-flow aerofoil sections. Proceedings 1st European Forum on Laminar

Flow Technology, pp. 175-183, Hamburg, Germany, DGLR, AAAF, RAeS, March 16-18 (1992)

[4] N. Qin, Y. Zhu, and S. T. Shaw, Numerical Study of Active Shock Control for Transonic aerodynamics, *International Journal of Numerical Methods for Heat & Fluid Flow*, Vol. 14 No. 4, pp 444 – 466, 2004.

[5] D. S. Lee, *Uncertainty Based Multiobjective and Multidisciplinary Design Optimization in Aerospace Engineering*, The Univ. of Sydney, Sydney, NSW, Australia, Section 10.7, p.p. 348-370, (2008)

[6] D. S. Lee, L. F. Gonzalez, J. Periaux, and K. Srinivas, Hybrid-Game Strategies Coupled to Evolutionary Algorithms for Robust Multidisciplinary Design Optimization in Aerospace Engineering. *IEEE Trans. Evolutionary Computation*, TEVC-00213-2009. (Accepted)

[7] J. Periaux, D. S. Lee, L. F. Gonzalez, and K. Srinivas, Fast Reconstruction of Aerodynamic Shapes using Evolutionary Algorithms and Virtual Nash Strategies in a CFD Design Environment, *Special Issue Journal of Computational and Applied Mathematics* (JCAM). Vol. 232. Issue 1, pages 61-71, ISSN 0377-0427, (2009)

[8] N. Hansen, A. Ostermeier, Completely Derandomized Self-Adaptation in Evolution Strategies. *Evolutionary Computation*, 9(2), pp. 159-195, (2001)

[9] J. Wakunda, A. Zell, Median-selection for parallel steady-state evolution strategies. In Marc Schoenauer, Kalyanmoy Deb, Günter Rudolph, Xin Yao, Evelyne Lutton, Juan Julian Merelo, and Hans-Paul Schwefel, editors, *Parallel Problem Solving from Nature – PPSN VI*, pages 405–414, Berlin, Springer, (2000)

[10] D. A. Van Veldhuizen, J. B. Zydallis, G.B. Lamont, Considerations in Engineering Parallel Multiobjective Evolutionary Algorithms, *IEEE Transactions on Evolutionary Computation*, Vol. 7, No. 2, pp. 144-17, (2003)

[11] M. Sefrioui, J. Périaux, A Hierarchical Genetic Algorithm Using Multiple Models for Optimization. In M. Schoenauer, K. Deb, G. Rudolph, X. Yao, E. Lutton, J.J. Merelo and H.-P. Schwefel, editors, *Parallel Problem Solving from Nature*, PPSN VI, pages 879-888, Springer, (2000)

[12] D. S. Lee, L. F. Gonzalez, and E. J. Whitney, *Multi-objective, Multidisciplinary Multi-fidelity Design tool: HAPMOEA – User Guide*, Appendix –I, D.S. Lee, *Uncertainty Based Multiobjective and Multidisciplinary Design Optimization in Aerospace Engineering*, The Univ. of Sydney, Sydney, NSW, Australia. (2007)

[13] M. Drela, A User's Guide to MSES 2.95. MIT Computational Aerospace Sciences Laboratory, September (1996)

[14] P. H. Cook, M. A. McDonald, M. C. P. Firmin, Aerofoil RAE 2822 – Pressure Distributions, and Boundary Layer and Wake Measurements, Experimental Data Base for Computer Program Assessment, AGARD Report AR 138, (1979)